Effect of phase change material in cross flow and jet impingement cooling techniques used in heat sink for electronics application

Deerajkumar Parthipan, Babu Dharmalingam, Somasundharam Sankaran & Deepakkumar Rajagopal

Taylor & Francis
Taylor & Francis Group

Check for updates

Effect of phase change material in cross flow and jet impingement cooling techniques used in heat sink for electronics application

Deerajkumar Parthipan[a], Babu Dharmalingam[b], Somasundharam Sankaran[c], and Deepakkumar Rajagopal[a] (iD)

[a]Department of Thermal and Energy Engineering, School of Mechanical Engineering, Vellore Institute of Technology, India; [b]Department of Mechanical Engineering, College of Engineering, Guindy (CEG), Anna University, Chennai, India; [c]Institute for Energy Studies, College of Engineering, Guindy (CEG), Anna University, Chennai, India

ABSTRACT

This article presents the results of numerical investigation on comparison between two different cooling techniques namely cross flow and jet impingement cooling techniques used in heat sinks for the electronic components. Pin fin heat sink with and without phase change material (PCM) are considered for the investigation. The main focus of this research is to reduce the peak operating temperature of electronic component and pressure drop and to increase the Nusselt number of the heat sinks. Computational fluid Dynamics (CFD) tool is used to model and investigate the heat transfer characteristics across the heat sink. It is found that the cross flow shows superior thermal characteristics compared to jet impingement method due to which the base temperatures of pin fins in cross flow is at an average temperature of 14.5° C lower than that of jet impingement. Furthermore, the use of PCM significantly reduces the operating temperature of the pin fins by an average temperature of 7.5 °C for cross flow and 6.1 °C for jet impingement flow techniques.

1. Introduction

The rapid development of electronic technologies has led to the rapid growth of electronic sector resulting in extremely high-power densities which result in substantial heat generation. This posed a new challenge to engineers on efficient rate of heat removal from the electronic chips so as to operate it within permissible limit. The main challenge is to efficiently remove generated heat, thereby to maintain the operating temperature within the limit. Furthermore, when components (e.g. transistors) become more integrated, heat generation on chip or device increases, which is harder to handle using traditional cooling strategies. On the other hand, the growth of electronics industries facing a big challenge of high-power densities that arise as a result of large-scale integration (LSI) of chips. This performance of electronic component reduces due to high-power density, also affects the lifetime of electronic components. New and advanced technologies lead to miniaturization of electronic devices with high energy densities due to high demand for better performance. Traditional cooling methods are lagging behind due to the aforesaid challenges and has low heat transfer coefficients (HTC), which brings up a demand of novel

Nomenclature

q''	Heat flux (W/m^2)	h	Enthalpy (J/kg)
E	Electrical power input (W)	$\dot{V}$	Volumetric flow rate (m^3/s)
A_b	Contact area of heat sink with heat generating device (m^2)	S_h	Energy generation rate per unit volume (J/m^3)
$\bar{Nu}$	Nusselt number $= \frac{q'' D_h}{k_{air}\left(T_w - \frac{T_{in}+T_{out}}{2}\right)}$	A	Area of channel (m^2)
d_h	Hydraulic diameter	P_c	Perimeter of channel (m)
k_{air}	Thermal conductivity of air (W/mK)	A_{fin}	Surface area of fin (m^2)
T_w	Average base plate temperature (°C)	n	Number of fins
$\bar{h}$	Convective heat transfer coefficient (W/m^{2}K) $= \frac{Nu.k_{air}}{D_h}$	μ	Dynamic viscosity (Ns/m^2)
		ψ	Volumetric fraction of PCM
Re	Reynolds number $= \frac{\rho u_0 D_h}{\mu}$	W	Width of fins (m)
ρ	Density (kg/m^3)	L	Length of fins (m)
u	Velocity (m/s)	D	Diameter of fins (m)
P_p	Pumping power (W) $= \Delta P.\dot{V}$	H	Height of fins (m)

technologies and cooling techniques for this purpose. The heat transfer mechanisms broadly classify the conventional cooling techniques into four categories, namely liquid evaporation, free convection and radiation, forced convective air cooling and forced convective liquid cooling. The most efficient of these traditional approaches is liquid evaporation, although forced air convection is most extensively utilized in cooling of CPUs. As the heat flux removal rate of forced convection of air is low, liquid evaporation or forced convection of liquid are preferred in many situations. Direct liquid injection cooling also has a greater heat transfer coefficient, meaning that the microchip surface temperature increases less than the fluid coolant temperature. In addition, when compared to air-cooling, this cooling provides improved chip temperature consistency. The advantages, limitations and features of traditional cooling systems are listed in Table 1.

Among the above-mentioned methods, heat sink is a passive heat exchanger that transfers the heat generated by an electronic device (chip) to a low temperature fluid medium. The main role of heat sink is to maximize the surface area of contact between electronic chips and the surrounding cooling medium. This is usually done by providing an extended surface called fins on the base of electronic chips. The design of heat sink is to optimize the parameters such that to reduce the operating temperature and pressure drop across the heat sink. In electronics cooling

Table 1. Cooling technologies [1].

Technology	Features	Advantages	Disadvantages	Cost
Free Convection	For low heat flux.	High reliability, low cost and noise free	Less heat removal rate, high heat transfer surface area.	Very cheap comparatively
Forced air convection	Requires fan for flow, replacement of free convection.	Highly Reliable and low maintenance. Used for cooling of large entities such as Data centers.	Low HTC, noise.	Costlier as compared to free convection.
Forced liquid convection	Cooling through flowing liquids, requires pumps and water is mostly used.	Higher Heat transfer coefficient compared to forced air convection, this method is used by heat exchangers.	Main application is not electronics cooling specially for small scale devices,	High cost due to infrastructure.
Liquid evaporation	Uses change of phase technique for cooling.	Highest HTC for heat removal, works good in arid climate	In hot, humid weather, it's not a good idea to use small electronic equipment.	Increased heating, installation, and maintenance costs.

applications, the phase change material (PCM) plays a major role due to its effective thermal management. The electronic components can be more powerful and compact while imposing PCM as a cooling agent. Cross flow cooling and Jet impingement techniques are two commonly known methods, they have different cooling mechanism across the heat sink. The cross-flow technique provides uniform cooling, suitable in low space requirement and larger heat distribution area, the lower heat transfer coefficient is a limitation in this technique. The Jet impingement cooling technique induce higher flow turbulence, result in higher convective heat transfer coefficient, nonuniform heat dissipation is limitation of this technique. The significance of PCM on the respective cooling methods may differ w.r.t. different flow conditions. So, the present study focused on the to compare the performance of heat sink with and without PCM using cross flow and jet impingement cooling techniques.

A review on recent literatures has been carried out to study the existing results on pin-fin type heat sinks without PCM or using PCM and their applications in the electronics cooling industry. The numerical experiments by Boukhanouf and Haddad [2] shows that the operating temperature is minimized by increasing the copper base plat thickness and replacing the base plate with vapor chamber of varying flow rates. A novel design of fins was introduced by Chu et al. [3] which includes triangular protrusions at the end of the fins. The results indicated that the novel design has less thermal resistance than that of conventional fins. It is also discussed that with protrusion angle greater than $45°$, the maximum temperature is reduced significantly. The effect of carbon nano tube microchannels on thermal characteristics with varying fluid and flow velocity has been studied by Rashid et al. [4]. The maximum temperature, heat extracted and thermal stress on fins with different geometries and orientations is analyzed. A rectangular and circular cross section of the fins in an array of 1D and 2D, different fluids (water and glycol) were considered in the study. The results concluded that the most efficient was the circular pin fin in case of both the working fluids and also increase in fluid velocity results in lower temperatures at any given configuration. Bahiraei et al. [5] investigated an alternate graphene based working nanofluid, in which a comparative study among different nano fluid concentrations, fin geometry and flow velocities has been studied. In their study, the authors reported the thermal resistance, pumping power, temperature uniformity, variation of fin temperature and convective coefficient. It was concluded that the maximum operating temperature reduces with increase in particle fraction of graphene and flow velocity, increases uniformity in temperature distribution and also reduces thermal resistance.

Freegah et al. [6] considered different types of fin geometries which includes filleted and non-filleted fins, symmetrical semicircle and corrugated semicircle on fins. The design was further optimized by reducing the pitch of the semicircle protrusions as well as hollow semicircle protrusions and further studies were carried out. It was concluded that plate type heat sinks with perforated round pins in a vertical parallel flow arrangement was the most efficient configuration among all examined designs. Sarma et al. [7] conducted a comparative study between regular and splayed heat sinks with different materials and configurations. The results show lower temperatures for splayed configurations when compared to regular pin fins. It was further concluded that hybrid splayed configuration provides the most efficient way of cooling while the regular aluminum pin fins the least. Various pin fin geometrical arrangements such as zig zag, slanted mirror, fluted, staggered, custom pin fin was compared for their thermal efficiencies by Kulkarni and Dotihal [8]. The results show that the slanted mirror pin fins are the best configuration, since they provide high Nusselt number, low pressure drop and lower temperatures as compared to other designs. Kim [9] performed a comparative analysis between the thermal characteristics of hollow hybrid fins (HHF), solid hybrid fins (SHF) and regular pin fins and their orientations. Results show that both HHF and SHF show better thermal characteristics than regular pin fins. Also, the hollow hybrid fins (HHF) show better performance than the other two. Li and Chen [10] demonstrated numerical and experimental techniques to explore the impact of the heat sink's

fin width and height on heat transfer at various Reynolds numbers. As the Reynolds number rises, the thermal resistance lowers. The ideal fin width of the heat sink is influenced by the Reynolds number. It increases in direct proportion to Reynolds number. Initially, increasing fin height improves the heat sink's thermal performance, however with further increase in fin height results in diminishing heat sink's performance.

Thermal characteristics of solid in fins and perforate pin fins in convective heat transfer have been studied by Chin et al. [11]. The pressure gradient across the heat sink diminishes as the number of perforations and perforation size increases. In every case, perforated pin fin array surpasses solid pin fin arrays thermal performance. Also, as number of perforations and the diameter of the perforations increase Nu number rises. The performance of elliptic, circular, and square cross-section pin fin heat sinks is compared, as well as the effect of fin density upon heat transfer performance is investigated by Yang et al. [12]. It was identified that the circular pin fins show greater HTC (Heat transfer coefficient) for inline arrangement in case of greater densities, while all three configurations show greater HTC in staggered arrangement. The circular fin shows smallest thermal resistance in inline arrangement. Longitudinal-wavy microchannel (LWC), straight rectangular cross section (SRC) and transversal microchannel (TWC) were designed and analyzed for their flow and heat transfer properties [13]. TWC shows superior thermal performance as compared to SRC whilst, LWC shows inferior performance. Though the HTC of TWC is less, it gets its superiority pertaining to the low pressure drop.

On the other hand, Rehman et al. [14] turned their interest at the operational time of PCM-based copper foam heat sinks in relation to certain temperatures, for both charging and discharging. Their findings revealed that a higher volume proportion of PCM resulting in a greater temperature drop. PCMs with low melting temperatures are appropriate for low heating loads & conversely. Low power levels are advised for the RT-35HC/Copper, and its greatest result is shown at low temperatures. RT-54HC/Copper foam, on the other hand, performs well at greater loads and temperatures. In an air jet impingement experiment, heat transfer increase for a range of heat sinks was investigated by Sheikh and Garimella [15]. Heat transfer coefficients were found to be higher with smaller pin diameters, ranging from 8 to 25% dependent on the nozzle size. Pin finned heat sinks was 2.4 to 9.2% more efficient than unpinned heat sinks, having tall pin fins with biggest aperture for jet impingement being the most efficient. Heat transfer increases by a factor of 7.5 (small unpinned heat sink) and 72 (big pinned heat sink) when compared to no heat sink (big pinned heat sink). Sivasankaran et al. [16] performed experimental analysis of parallel plate fin and crosscut fin with an asymmetrically placed heating element. The average heat transfer coefficient of parallel plate fins is higher than crosscut fins with many perforations. Variation of channel diameter to study the hydraulic and thermal properties of heat sink is carried out by Ghasemi et al. [17]. The findings of the experiments reveal that increasing the channel size lowers drop in pressure in the heat sink. Furthermore, the thermal resistance of a mini-channel heat sink which has a hydraulic diameter equal 4 mm is significantly lower than that of the mini-channel heat sinks which have hydraulic diameters of 6 and 8 mm. In comparison to other examples, heat sink with diameter equal to 4 mm greatly reduced heat sink temperatures, according to the measured data.

Mahmoud et al. [18] experimentally investigated the use of PCM with cross and parallel plate heat sinks and honeycomb structures. PCM can aid in lowering the heat sink's maximum temperature and heating rate. PCM, on the other side, has a slower cooling rate. Heat transmission to the PCM can be increased by increasing the number of fins on the heat sink, resulting in reduced heat sink heating rates. Lu and Vafai [19] performed a comparative analysis on microchannel heat sinks (MCHS), namely single layered (SL-MCHS), double layered (DL-MCHS), multi layered (ML-MCHS). The DL-MCHS and ML-MCHS show superior thermal characteristics as compared to SL-MCHS. In comparison to other systems, ML-MCHS significantly reduces temperature rise, thermal resistance, and pumping power. A numerical analysis was done by Pakrouh

et al. [20] to optimize the geometry of pin fin-based heat sinks and the PCM volume percentages to maximize the operational time. Different critical temperatures ranging from 50 to 80 °C were considered in this study. The optimum PCM percentage was found to be 16.6% for a 4mm thick fin while for a 2mm thick fin it was found to be 82.6%. Naphon et al. [21] carried out experimental investigation on jet impingement flow technique using nanofluids. The parameters that were investigated are nanofluid concentration, nozzle to heat sink distances and nozzle diameter with a varying mass flow rate of the nanofluid. The HTC increases as the nozzle diameter increase and the space between both the nozzle and fin decreases. The pressure decreases as the nozzle diameter is reduced and the distance between the nozzle and the fin is increased. Experimental analysis on fins with PCM named n -eicosane was carried out by Ali and Arshad [22]. Four configurations were selected which included no fin heat sink and heat sink with 2, 3 and 4mm fins. Power densities, latent heat, and thermal capacities are investigated over a range of heat flux values. The result indicates that the heat sink with the 3mm fins provides better thermal characteristics. Arshad et al. [23] presented an experimental study of round finned heat sinks for mobile devices. Paraffin wax is used as the PCM material and pin fins of diameters 2, 3, and 4mm are considered. Different volume fractions of PCM are also considered ranging from 0, 50 and 100% and it was concluded that 3mm finned heat sink shows superior thermal performance. Very recently, Shoujin Chang et al. [24] proposed a novel paraffin-fatty acid eutectic system for thermal management, experimentally investigated and reported the enhanced latent heat at the existing phase transition temperatures. Yao Hui et al. [25] experimentally investigated the jet impingement on a metal foam covered heated surface, observed increased heat transfer coefficient with increasing jet velocity.

From the previous literature, it is understood that the challenges faced in the field of electronics cooling has been increasing with miniaturization of electronic components using technologies such as VLSI. Heat sinks are mostly used in electronic system for better thermal management of the components. The application of PCM in heat sink provides better heat transfer, higher heat storage capacity and lower temperature fluctuation. The PCM absorb excessive heat generated from the electronics components, such that the system can be maintained in a stable operating temperature, leads to prolonged life to the components. The higher heat storage capacity of heat sink with PCM leads to compact and lightweight design. Moreover, the usage of PCM has become mandatory to avoid overheating of heat sink or to increase the time gap to reach the maximum operating temperature of heat sink from the normal room temperature. The various advanced analyzing techniques of thermal characteristics across the heat sink were explored. Also, it shed some light on the importance of further research on the cross flow and jet impingement techniques with PCM.

2. Problem statement

This study focused on optimizing the cooling strategy using cross flow and jet impingement methods and compare the thermal characteristics of pin fins. The thermal characteristic of pin fins under cross flow technique is compared with jet impingement flow techniques with respect to different flow conditions. Four set of simulations are carried out, namely (a) Cross flow without PCM (b) Cross flow with PCM (c) Jet impingement without PCM (d) Jet impingement with PCM. A circular fin with an array of 14 fins of 8 mm in diameter, 50 mm in length is considered for all the cases. The base plate length is 95 mm, its thickness is 3 mm. The pin fins are placed 25 mm apart from each other. As compared to plate fin, the pin fin provides better heat transfer co-efficient and lower pressure drop. In particular, the staggered arrangement of pin fin provides better thermal dissipation as compared to inline arrangement with some penalty in pressure drop. So, in the present work staggered pin fin is considered, the geometrical detail is taken from
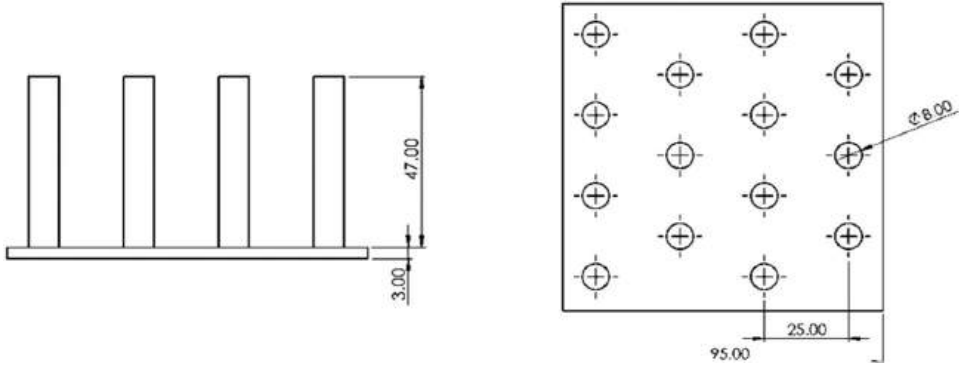
Figure 1. Two-dimensional representation of pin fin heat sink.

the experimental work of Chin et al. [11]. The two-dimensional representation of pin fin heat sink is given in Figure 1.

The thermal energy generated in the electronic chip is dissipated by convection, conduction, and radiation. The radiation heat transfer amounts only to 0.5% of the total heat transfer [11] due to small difference in temperature between pin fins and ambient environment. The conduction heat losses amount up to 1.1% of the total heat loss [11]. So, the convective heat transfer plays the major role in electronics cooling to dissipate all the residual heat. But in case of PCM conduction and latent heat of the PCM plays a very crucial part in heat dissipation.

$$Q_{total \ without \ PCM} = Q_{conduction} + Q_{convection} + Q_{radiation} \tag{1}$$

$$Q_{total \ with \ PCM} = Q_{conduction} + Q_{convection} + Q_{radiation} + Q_{latent \ heat} \tag{2}$$

The PCM for a heat sink application works better depend on available space and the way of approaching of cooling medium interacting with heat sink base and fin surfaces. The "Cross Flow" and "Jet Impingement" are two different commonly used cooling techniques. The cooling requirements and constraints of the system decides the selection of these two cooling techniques. So, the effect of PCM on these techniques will be interesting study to understand the thermal characteristics of PCM in heat sink.

2.1. Computational domain of heat sink cooled by cross flow technique

In cross flow technique, the heat transfer fluid flow perpendicular to the heated surface that requires cooling. It is preferable due to its simplicity, low cost, and compatibility with various systems with a limitation to low heat flux applications. The geometric model for cross-flow technique consists of a rectangular channel of length 1050 mm with a breadth of 100 mm and height of 50 mm as shown in Figure 2. The inlet boundary of the channel is placed 697.5 mm away from the fin array to avoid the numerical error due to flow development, while the outlet is placed 257.5 mm downstream from the pin fins to ensure the outflow boundary condition such that the gradient across the boundary becomes nullified.

2.2. Computational domain of heat sink cooled by jet impingement technique

In jet impingement technique, a very high velocity jet is directed toward the heated surface, the continuous disturbance in the boundary layer result in higher convective heat transfer coefficient, preferred in high heat flux applications with the limitation of penalty in pressure drop. A box of dimensions $210 \times 210 \times 112$ mm is considered as a computational domain for jet impingement cooling method, where the pin fin is placed at the center of the computational domain. The
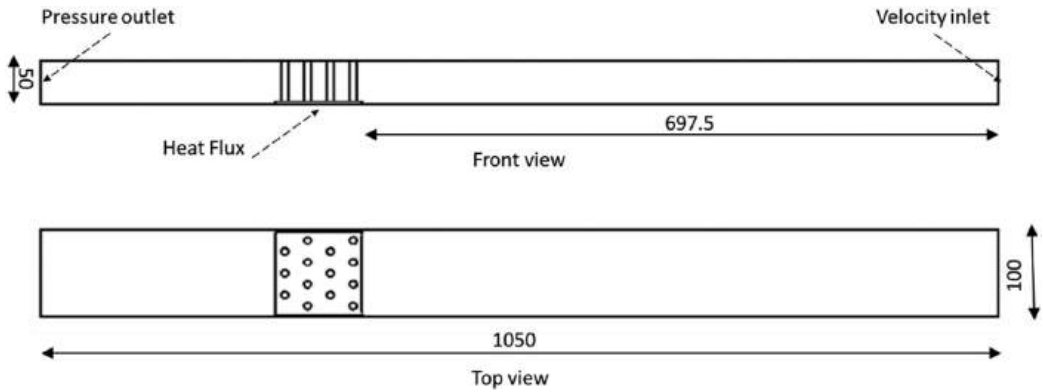
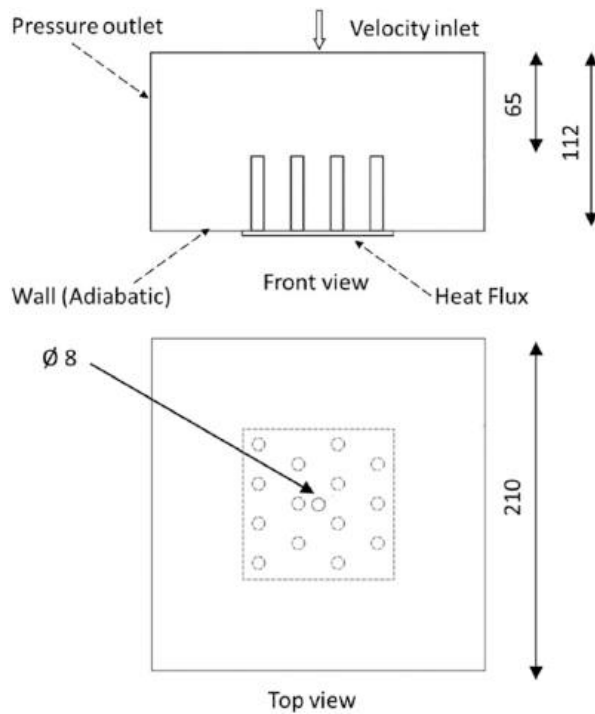Figure 2. Geometry of cross flow domain with appropriate boundary types.

Figure 3. Geometry of jet impingement domain with appropriate boundary types.

two-dimensional representation of the computational domain *via* front and top view is shown in Figures 3a and b, the direction of impingement is shown by arrow mark (Figure 3a). The orifice of diameter 8 mm is located at the center of the top surface of the computational domain, which is 65 mm above from the pin fin top surface.

2.3. Computational domain of heat sink cooled by PCM technique

In this case, the pin fin is surrounded by PCM material for better thermal characteristics. 50% of the volume is filled with phase changing material, due to which the convective heat transfer and
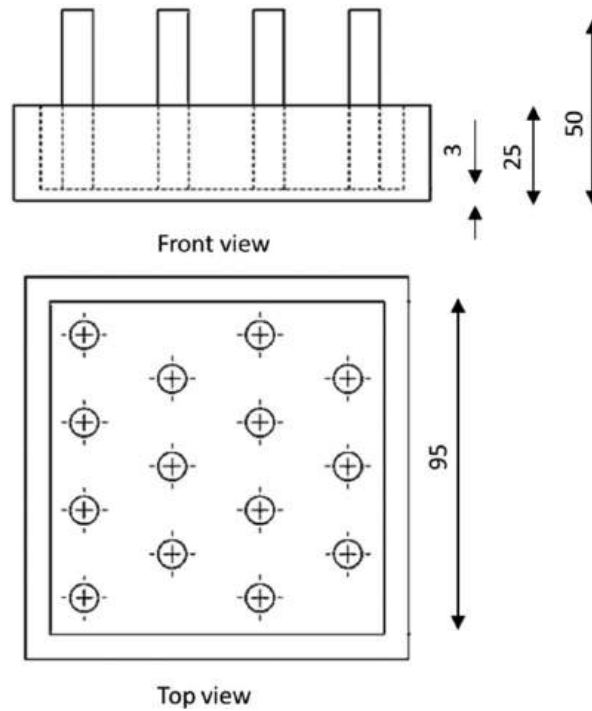
Figure 4. Geometry of heat sink with PCM.

the latent heat of the PCM contributes toward the cooling of the heat sink. The geometry considered in the study is given in the Figure 4.

3. Solution methodology

CFD technique has been adopted to solve the conjugate heat transfer characteristics across the heat sink and surrounded air. The computation domain is modeled and discretized into finite number of control volumes and the governing equations are solved with appropriate boundary conditions assigned on the domain surface. Through the field variables, the required engineering parameters are derived and reported for the analysis of the flow and heat transfer characteristics.

3.1. Domain discretization

'Solidwork' software tool is used for the three-dimensional geometrical modeling of pin fin heat sink with closed computational domain. The computational domain is discretized using 'ICEM CFD' software tool, the grid quality is ensured above 0.6 based on the quality criterion in ICEM CFD for all the cases studied. As the fluid flow and structure interaction involves a complex geometry, an unstructured grid method is employed to discretize the domain. Figures 5–7 shows the schematic representation of the grids of cross flow, jet impingement and PCM cooling techniques respectively. The cross-flow cooling technique (Figure 5) involves a flow inlet and exit across (i.e. perpendicular to) the pin fins of heat sink, the computational domain consists of heat sink enclosed with a rectangular channel. The channel is extended in both the upstream and downstream of the heat sink. The upstream and downstream regions are discretized with coarse grid as these regions undergoes lower velocity, pressure and temperature gradients as compared to the region very near to the heat sink. To accurately capture the gradients, the grid is finer near to the
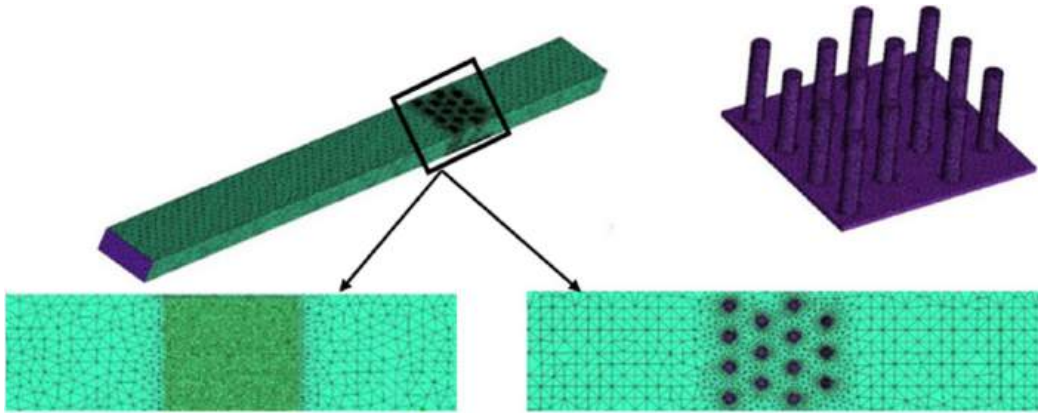
Figure 5. Schematic representation of grid in cross flow cooling technique (number of finite control volumes = 781,924).
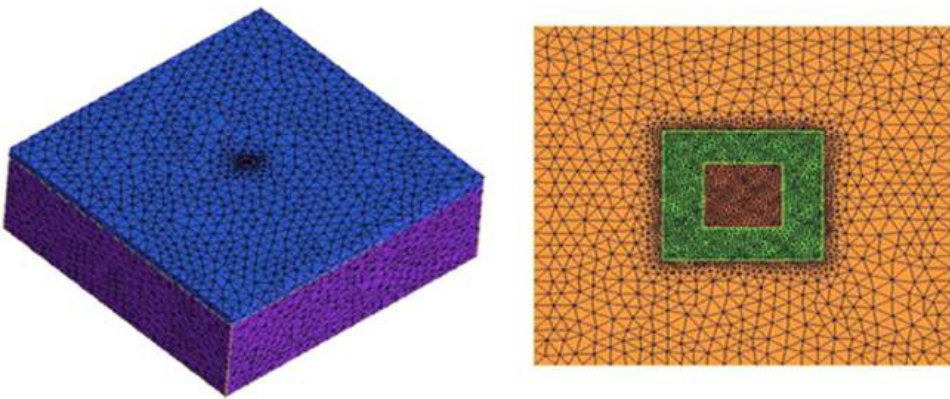

Figure 6. Schematic representation of grid in jet impingement cooling technique (number of finite control volumes = 482,510).

fin and base surface of the heat sink. The jet impingement cooling technique (Figure 6) involves a high velocity jet strikes perpendicular to the heat sink base. So, the computational domain does not require the prolonged channel length, whereas to impose the pressure outlet boundary, an imaginary square type domain is extended from the base to top of the heat sink. As discussed earlier, to capture the gradients, a fine grid is generated near to the heat sink surface, a coarse grid is generated in the extended domain. As, the size of the computational domain is less than the cross-flow technique, the number of finite volumes generated is lower (482,510) than the cross-flow technique (781,924). The PCM cooling technique (Figure 7) uses only PCM as a cooling medium, it does not contain inlet and outlet boundaries. So, heat sink with PCM is considered as a computational domain, an extended domain is not necessary in this technique. As the domain size further decreases, the number of finite volumes generated is further decreased (134,866) in this technique.

3.2. Grid independence study

In the preprocessor phase, Ansys ICEM CFD is used to discretize the three-dimensional computational domain. Since, the computational domain contains the interaction of various shapes, causes
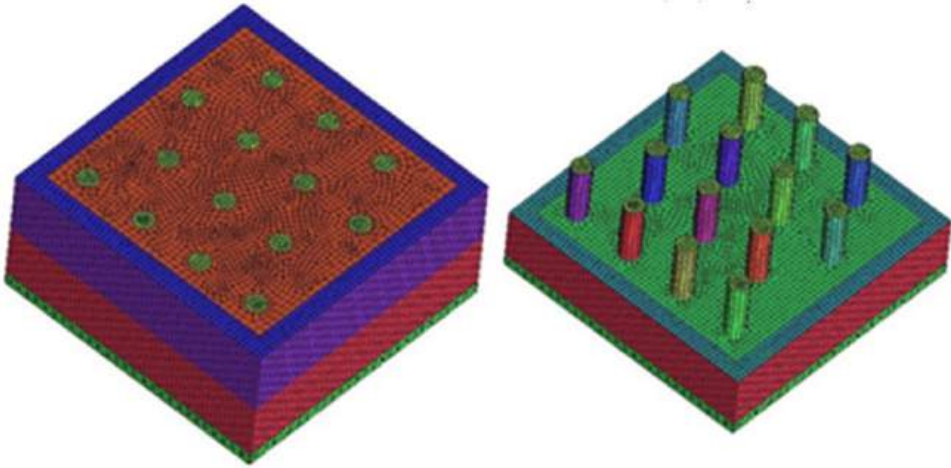
Figure 7. Schematic representation of grid in PCM cooling technique (number of finite control volumes = 134,866).
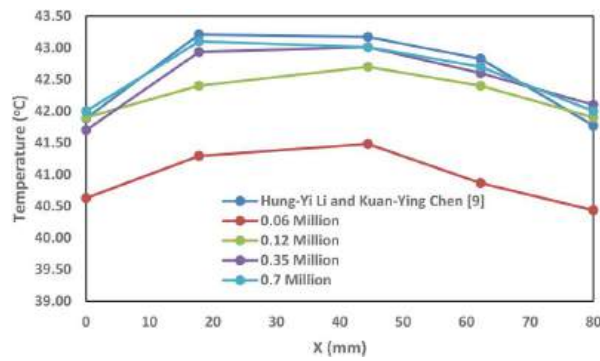

Figure 8. Variation of temperature with respect to grid size.

to a complex structure, the computational domain is discretized using tetrahedral unstructured mesh. The effect of grid size on the temperature distribution along the fin is monitored and the results are reported in Figure 8. The finest grid set chosen resulted in around 0.7 million control volumes in the computational domain whereas the coarse mesh corresponds to 0.06 million control volumes. The error for 0.06 million cells is 3.8% while that of other grid sets are less than 1%. Hence, a grid size of 0.12 million was chosen for the further study to optimize the accuracy and computation cost. The minimum quality of the element in overall mesh is maintained 0.6 based on the ICEM CFD quality criterion.

3.3. Turbulence modelling and boundary conditions

The continuity equation in three dimensional, steady, incompressible flow and energy equation is solved using the finite volume-based solver Ansys Fluent. The realizable $k - \epsilon$ turbulence model is used with standard wall functions [11], which predicts spreading rate better particularly in jet flows. SIMPLEC algorithm was used for the coupling of velocity and pressure along with a second order discretization scheme. The convergence criteria of 10^{-6} is taken for all the equations to be converged.

Continuity equation

$$\nabla.\left(p\overrightarrow{v}\right) = 0 \tag{3}$$

Momentum equation

$$\rho\overrightarrow{v}.\nabla\overrightarrow{v} = \mu\nabla^2\overrightarrow{v} - \nabla P \tag{4}$$

Energy equation

$$\rho c_p \nabla.\left(\overrightarrow{v}T\right) = \nabla.(k\nabla T) \tag{5}$$

k-ϵ realizable transport equations

$$\frac{\partial}{\partial x_j}(\rho\kappa u_j) = \frac{\partial}{\partial x_j}\left[\left(\mu + \frac{\mu_t}{\sigma_k}\right)\frac{\partial\kappa}{\partial x_j}\right] + G_\kappa + G_b + \rho_\epsilon + Y_M \tag{6}$$

$$\frac{\partial}{\partial x_j}(\rho\epsilon u_j) = \frac{\partial}{\partial x_j}\left[\left(\mu + \frac{\mu_t}{\sigma_k}\right)\frac{\partial\epsilon}{\partial x_j}\right] - \rho C_2\frac{\epsilon^2}{\kappa + \sqrt{\vartheta\epsilon}} + C_{1\epsilon}\frac{\epsilon}{\kappa}C_{3\epsilon}G_b \tag{7}$$

3.4. Boundary condition for cross flow technique

A heat flux boundary is considered at the base of the pin fin with the value of 5903 W/m^2. A k-ϵ turbulence model was chosen with standard wall functions. The hydraulic diameter and turbulence intensity is taken as 0.067 m and 10% respectively. The pin fin walls and the channel walls are assumed to be no-slip wall boundary conditions. The adiabatic boundary condition is assumed for all other remaining walls except the base of the fins. The schematic of the boundary conditions for cross flow cooling is given in Figure 2.

3.5. Boundary condition for jet impingement cooling

The schematic of the jet impingement domain with appropriate boundary conditions is given in Figure 3. The heat flux is same as the cross-flow setup, assigned a value of 5903 W/m^2 at the base of the pin fin. The velocity inlet boundary condition is assigned at the orifice, all the other faces are considered as pressure outlets. The base surface of the computational domain is considered as an adiabatic wall boundary.

3.6. Numerical setup for PCM model

A VOF (Volume of fluid) model is used for solving the PCM model without mixing of two fluids, which in this case paraffin wax is considered as PCM. A time dependent transient simulation is performed to analyze the thermal characteristics and the latent heat phase of pin fins with PCM. A time step of 10 s was considered and the total number of time steps were taken to be 540, which makes the flow time of 90 min. The governing equations for this model are given below.
Continuity equation

$$\frac{D\alpha}{Dt} = 0 \tag{8}$$

where, α is fluid's volume fraction in the domain.
Momentum equation

$$\rho\frac{D\overrightarrow{v}}{Dt} = -\nabla P + \mu\nabla^2\overrightarrow{v} + \overrightarrow{S} \tag{9}$$

$\overrightarrow{S}$ is defined as the momentum sink due to reduced amount of porosity in the mushy zone. The equation defining $\overrightarrow{S}$ is given by:

$$\overrightarrow{S} = -\frac{C(1-\gamma)^2}{(\gamma^3 + \epsilon)}\overrightarrow{v} \tag{10}$$

where C is the mushy zone constant which is taken to be 10^5 for this case [20].

The density of PCM in liquid phase can be expressed as

$$\rho = \frac{\rho_l}{\beta(T - T_l) + 1} \tag{11}$$

The value of β is taken to be 0.001 according to the research done by [26].

Dynamic viscosity of PCM with respect to temperature can be defined as

$$\mu = 0.001 \times \exp\left(-4.25 + \frac{1790}{T}\right) \tag{12}$$

The volumetric fraction (ψ) of the PCM is defined as the ratio of the PCM volume to the total volumetric capacity of the heat sink. It can be calculated using the equation

$$\psi = \frac{v_{PCM}}{v_s - v_f} \tag{13}$$

The material properties of PCM are given in Table 2.

3.7. Data reduction

The convective thermal energy that is dissipated is given in Eq. (14).

$$q'' = \frac{0.984\ E}{A_b} \tag{14}$$

where, q'' is the convective thermal energy, E is the electrical power input due to which the heat is generated and A_b is the contact area of the fin with the heat generating device.

The solid heat conduction equation is given by the equation.

$$\frac{\partial}{\partial x}(\rho h) = \frac{\partial}{\partial x_i}\left(k\frac{\partial T}{\partial x_i}\right) + S_h \tag{15}$$

The hydraulic diameter for the jet impingement flow is taken to be equal to orifice diameter i.e. 8 mm while that for the cross flow it is calculated using the equation.

$$D_h = \frac{4A}{P_c} \tag{16}$$

Table 2. Material properties of paraffin wax PCM [23].

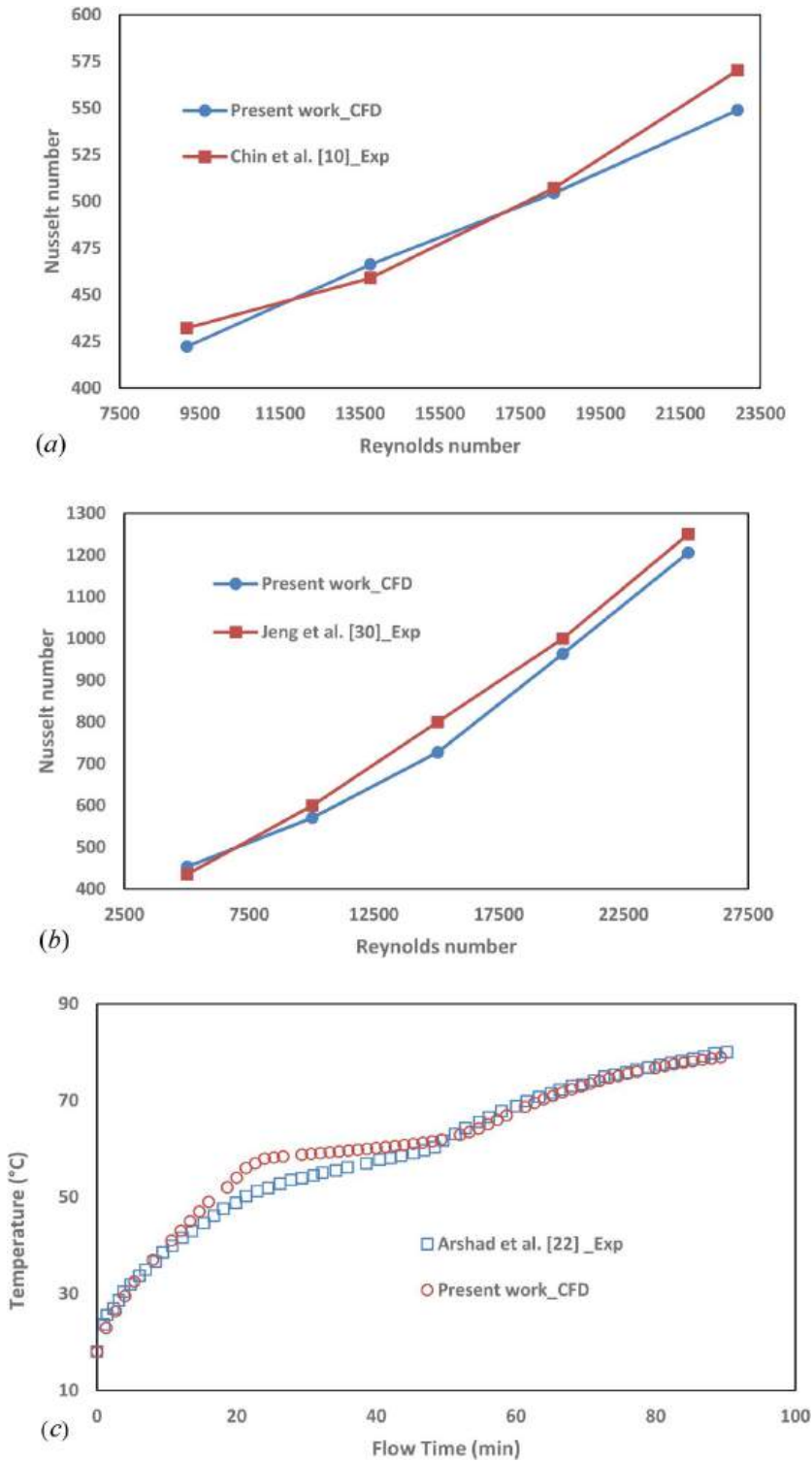| Properties	Values
Density (kg/m^3)	880 (solid)
	790 (liquid)
Thermal conductivity (W/mK)	0.212 (solid)
	0.167 (liquid)
Viscosity (kg/ms)	0.00252
C$_p$ Specific heat (J/kg.K)	2800
Thermal expansion coeff. (K^{-1})	0.001
Pure solvent melting heat (J/kg)	173,600
Solidus temperature (K)	329
Liquidus temperature (K)	331

Figure 9. Validation results of (a) cross flow (b) jet impingement and (c) PCM techniques.

Table 3. Validation of cross flow.

Reynolds no.	Nu (present work) [11]	Nu (experiment)	Error %
9173.46	422.23	445	−2.29
13760.19	466.21	485	1.588
18346.93	504.46	530	−0.52
22933.66	548.86	605	−3.73

Table 4. Validation of jet impingement flow.

Reynolds no.	Nu (present)	Nu (experiment) [31]	Error %
5019	453.11	435	4.13
10039	570.58	600	4.9
15058	727.26	800	9.1
20077	963.56	1000	3.64
25096	1205.56	1250	3.55

The total area of heat transfer for the fins can be expressed as

$$A_{fin} = WL + \pi Dn \left(H - \frac{D}{4} \right) \tag{17}$$

4. Results and discussion

This section presents the results of thermal characteristics among the cooling of pin fin heat sinks in cross flow and jet impingement flow techniques. In the Sect. 4.1, the CFD model is validated against the existing experimental and numerical results. Then, similar models are simulated for cross flow and jet impingement with respect to Reynolds number.

4.1. Validation of cross flow model

In this cross-flow model, the heat sink is placed in an imaginary rectangular channel act as a computational domain, which has shorter upstream length and longer downstream length with respect to heat sink. The significance of upstream and downstream extension on capturing the flow characteristics can be found in the previous literatures [27–30]. The aim of this validation is to find out the ability of CFD model to capture the Nusselt number values of solid pin fins obtained by experimentation. The model is successfully validated against experimental results of Chin et al. [11] with a maximum error of 3.7%. Figure 9*a* shows the comparison graph with varying Reynolds number. Table 3 shows the values obtained using CFD, experimental values and the error between the two values.

4.2. Validation of jet impingement model

The jet impingement CFD model is validated with experimental results of Jeng et al. [31]. It is to be noted that CFD model predicts closer to experimental results, the average and maximum deviation in Nusselt number is 5.06 and 9.1% respectively. The comparison is presented in Figure 9*b* and the values are given in Table 4.

4.3. Validation for PCM model

A preliminary study has been conducted by Deeraj Kumar and Deepakkumar [32] to compare the cross flow and jet impingement cooling techniques without PCM. This present work focused on to identify the effect of PCM. Arshad et al. [23] compared the effects of PCM percentage on
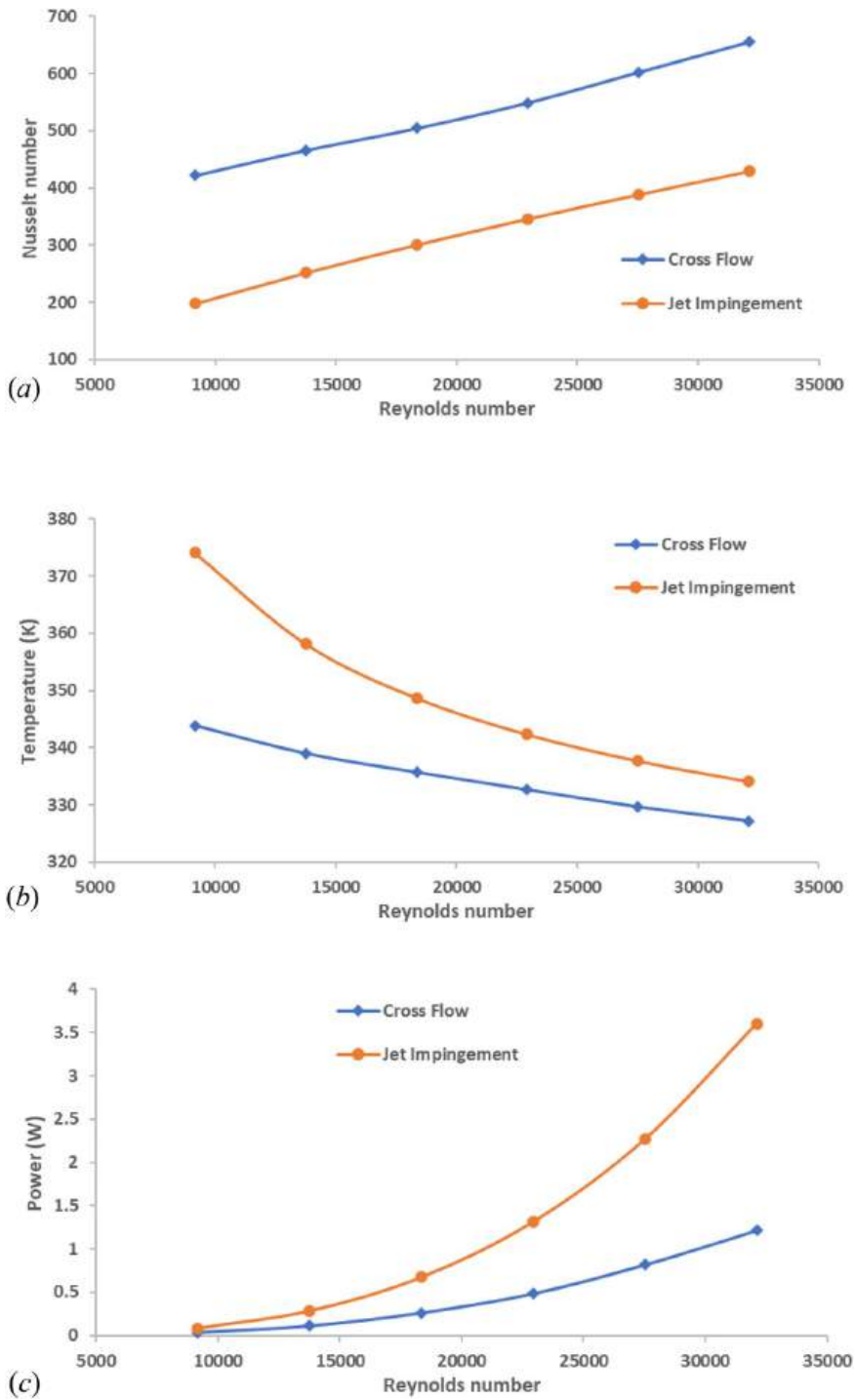
Figure 10. Comparison of (a) Nusselt number (b) base temperature (c) pumping power (d) pressure drop (e) thermal resistance between cross flow and jet impingement cooling.
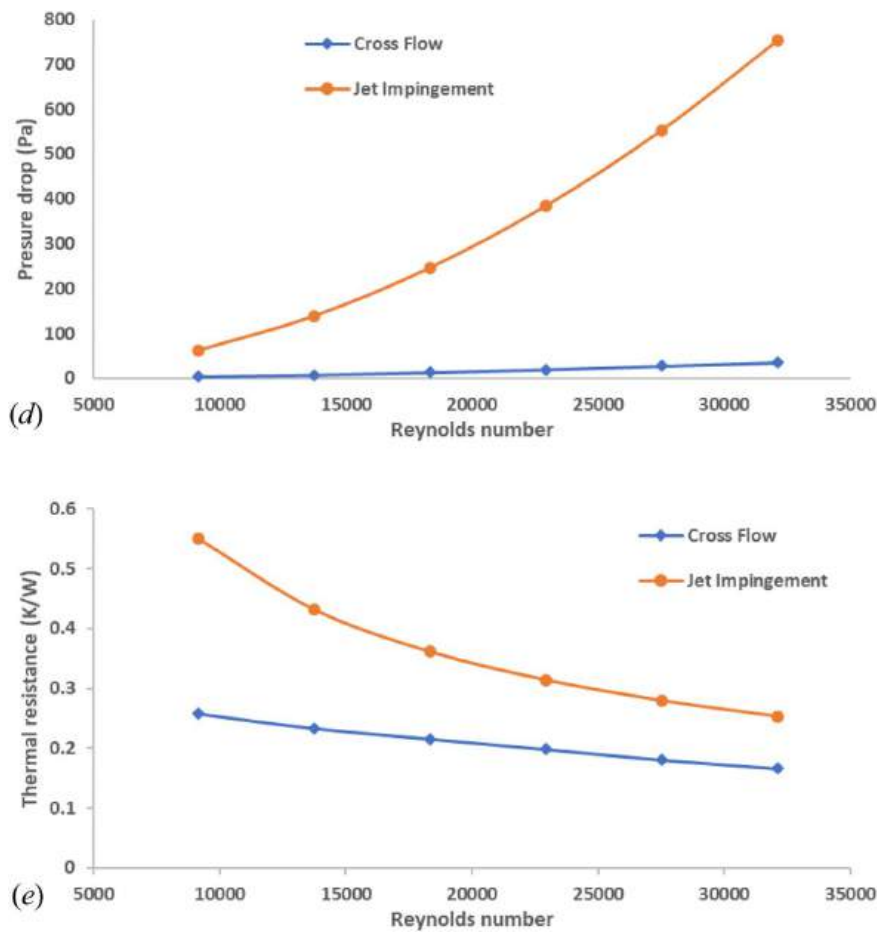
Figure 10. Continued.

the base temperature of heat sinks using experimental methods. The data from this research is used as validation benchmark for PCM model. The CFD model is validated successfully. The flow time considered for the transient simulation was 90 min and the PCM volumetric percentage was taken to be 50%. Figure 9c shows the comparative results between the experimental data and CFD simulation.

4.4. Comparison of cross flow and jet impingement cooling without phase change material

This study is carried out to compare the thermal characteristics of pin fins under different flow conditions. First the Nusselt number values for both cross flow as well as jet impingement is studied for varying Reynolds number. A Reynolds number varying from 9000 to 32,000 was considered for the study. The Nusselt number comparison results are shown in Figure 10a. The Nusselt number is significantly high for cross flow conditions than that of jet impingement for the same Reynolds number values. The base temperatures also show a similar trend with jet impingement having higher base temperatures as compared to the cross-flow technique. The comparison for the base temperatures is given in Figure 10b.
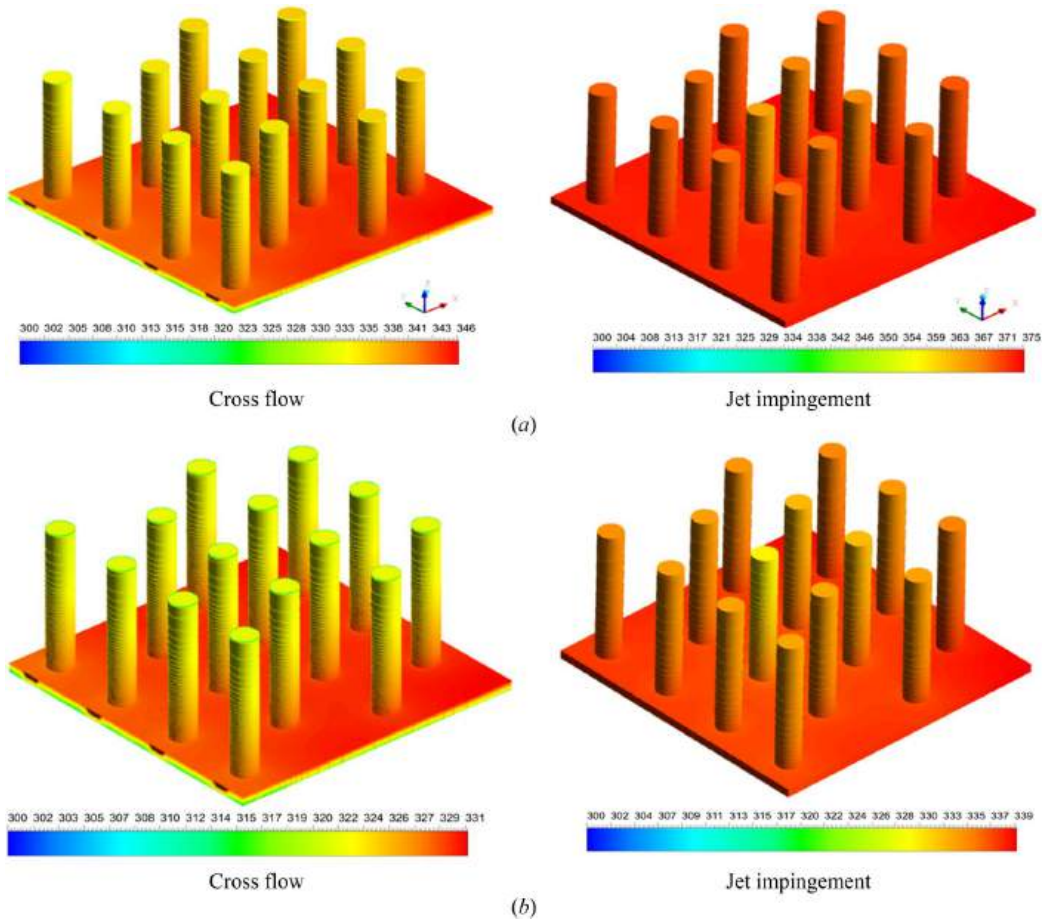
Figure 11. Temperature contour of cross flow and jet impingement (a) Re $=$ 9000 (b) Re $=$32000.

The pressure drop values are also compared for both the flows which is presented in Figure 10c. The pressure drop for cross flow is significantly less than that of jet impingement which indicates better thermal characteristics. The pressure drop increases with increasing Reynolds number in both the cases, but the magnitude of increase is much higher in the jet impingement technique. With this we can say that the thermal performance of the cross-flow technique is better, but we also have to consider the pumping power required to operate the cooling system. The comparison of pumping power is shown in Figure 10d. The pumping power of the jet impingement method is more due to the greater pressure drop as compared to the cross flow, which indicates inferior thermal performance. From these results we can conclude that using cross flow method is more efficient and economical than the jet impingement technique. The cross flow provides better Nusselt number values for the respective Reynolds number than the jet impingement methods, while keeping the pressure drop and the pumping power low. The operating base temperature is also reduced by using cross flow technique over the jet impingement one. Thermal resistance is also compared between these two methods, which is shown in Figure 10e. There is no significant difference in thermal resistance, even though the pressure drop in jet impingement is high.

Figures 11a, b shows the comparison of temperature contours between cross flow and jet impingement cooling techniques of the fins at Reynolds number 9000 and 32000 respectively. The cross flow gives lower fin temperatures in every case. Figures 12a, b shows velocity contour
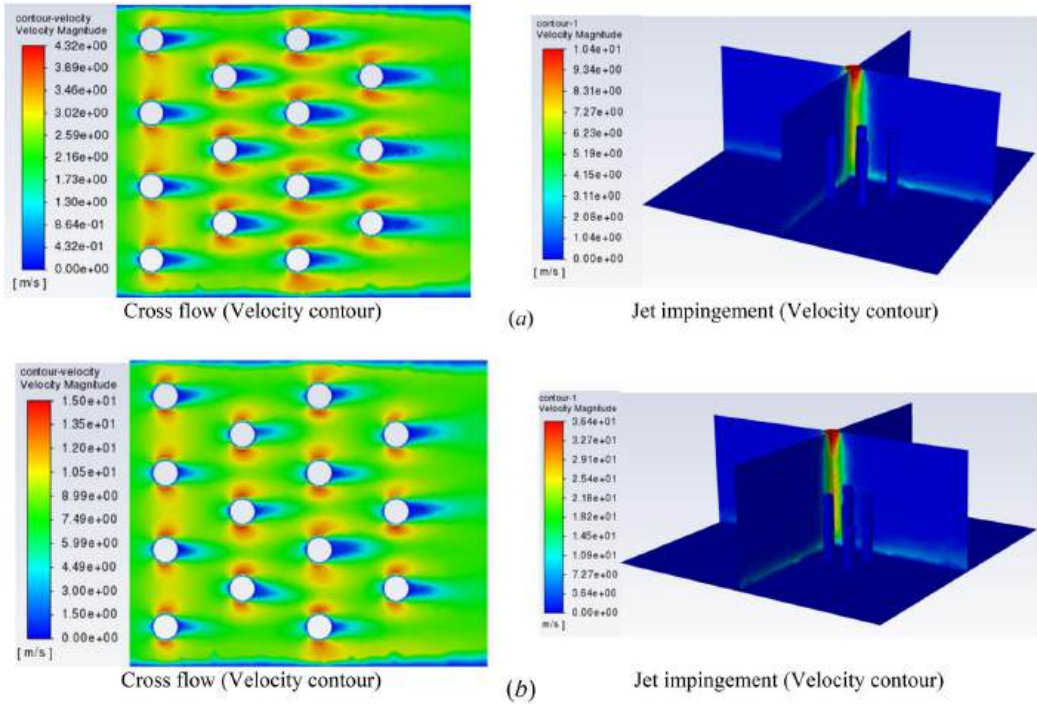
Figure 12. Velocity contour of cross flow 20 mm from the base and jet impingement (a) Re = 9000 (b) Re = 32000.

on a plane 20mm above the base for cross flow at two different Reynolds number 9000 and 32000 respectively. From the velocity contour it is observed that the fins located at the downstream experiences low pressure, result in increased wake region behind the fins, thus the convective heat transfer reduces from the fin surface. Moreover, the temperature gradient is less in the fins located at the downstream as compared to upstream fins, thus the base temperature of fins located at the downstream experiences high as compared to upstream fins. In Jet impingement method, it is observed from the contour the air jet mainly focused at the center of the heat sink base, the interaction is less significant in other heat transfer surfaces. Thus, the temperature near the fins is higher at a lower Reynolds number. The above inference can be ensured from the velocity vector plot and path lines through the Figures 13a, b. Since the convective heat transfer coefficient of the Jet impingement method is low it can be seen that the operating temperature of the fins is higher than the cross-flow method. This is evidence that the cross-flow method provides better cooling characteristics than the jet impingement cooling method.

4.5. Comparison of cross flow and jet impingement cooling with phase change material

A comparative analysis was carried out to analyses the thermal characteristics of pin fins with 50% volume fraction of PCM under cross flow and jet impingement techniques. Figure 14a shows the base temperature comparison from Reynolds number ranging from 9000 to 32000 in crossflow. The base temperature reduces progressively from a lower Reynolds number to a higher Reynolds number, increased convective heat transfer coefficient due to increased velocity. Since, the max temperature does not exceed the liquidus temperature of the PCM, the latent heat of the PCM does not actively contribute toward the cooling of the Pin fin. But the usage of PCM has reduced the base temperature of the pin fin as compared to cross flow without PCM. We can observe a temperature drop of 9.5 degrees with an increasing Reynolds number from 9000 to
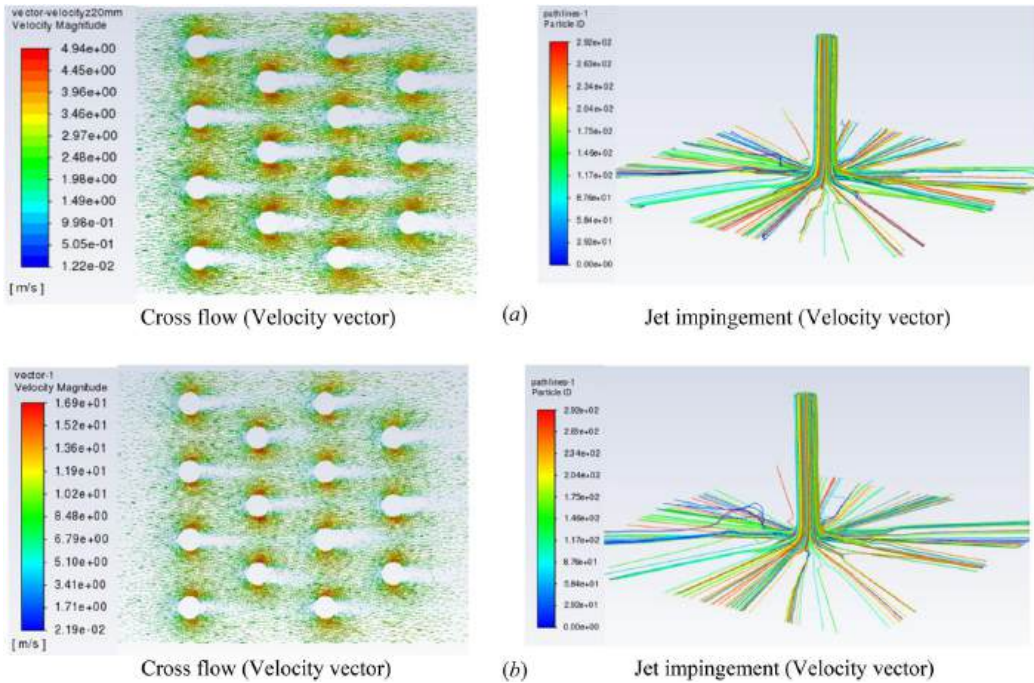
Figure 13. Velocity vector and path line for cross flow and jet impingement respectively at (a) Re = 9000 (b) Re = 32000.

32000. The base temperature comparison for Jet impingement using PCM is shown in Figure 14b. The peak temperature of the pin fin overshoots the liquidus temperature of the PCM, due to which the latent heat of the PCM comes to play. But the effect of latent heat disappears with Reynolds numbers greater than 23000, Due to increased convective heat transfer coefficient and reduced base temperatures. Since the base temperatures at higher Reynolds numbers fall within the liquidus temperature of the PCM, the difference between the base temperatures is not as significant as compared to that of lower Reynolds numbers. The difference between base temperatures at Reynolds number 9000 and 14000 is 10.2 °C while the difference between base temperatures at Reynolds number 28000 and 32000 is 2.12 °C. The total reduction in the temperature obtained by using jet impingement with PCM is 32.16 °C over the range of Reynolds number.

The time versus Nusselt number graph (Figures 14c, d) shows three different regions. In general, there is quite different in the trend for cross flow and jet impingement cooling methods. In the first region, where the temperature gradient between the heat sink surface and incoming cooling fluid is very high, the Nusselt number decreases rapidly with progress in time approximately for the initial 10 min, the sensible heat of PCM in solid state rises the base temperature. In the second region, where the temperature gradient remains less or almost constant w.r.t. Rynolds number, which is due to the latent heat of PCM makes no variation in the base temperature of heat sink. Further, in third region, the Nusselt number further decreases gradually with time, but the decrement is very less as compared to region 1. A significant decrement is observed only for jet impingement cooling method, particularly at low Reynolds number. This is due to sensible heat of PCM in liquid state rises the base temperature very high at low Reynolds number. In cross flow cooling technique, the incoming fluid effectively contact with base surface of the heat sink as compared to the jet impingement cooling, where the incoming jet only interacts with the center of the heat sink.

Figure 15 shows the comparison of base temperatures between cross flow and jet impingement with and without PCM at different Reynolds numbers. The difference between the max base temperature is prominent at lower Reynolds number and is reduced with increasing Reynolds
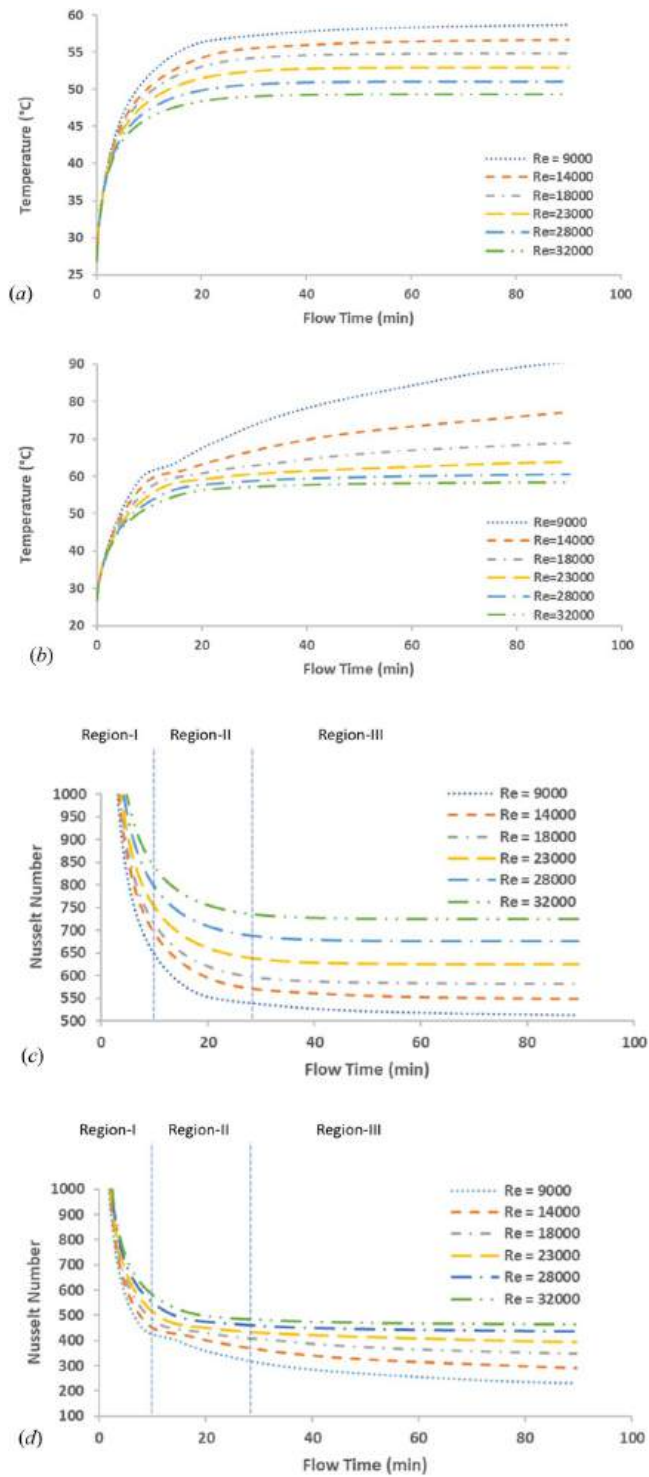
Figure 14. Effect of phase change material on (a) base temperature (cross flow) (b) base temperature (jet impingement) (c) Nusselt number (cross flow) (d) Nusselt number (jet impingement).
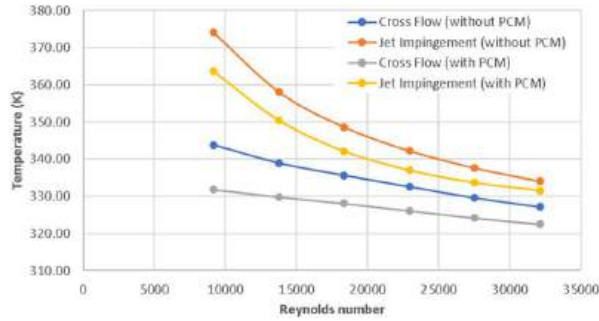
Figure 15. Comparison of base temperature with PCM.

number. But cross flow method shows better thermal characteristics as compared to jet impingement and keeps the base temperature lower throughout the Reynolds number range. The temperature difference between cross flow and jet impingement at Reynolds number 9000 is 31.9 °C, while the temperature difference at Reynolds number 32000 is 9 °C. This phenomenon is due to the higher liquidus temperature of paraffin wax which is chosen as the PCM material for the study. Since the convective heat transfer coefficient of cross flow is higher than that of the jet impingement method, the majority of the cooling takes place using convection, due to which the temperature stays below the liquidus temperature of the PCM. In jet impingement method the convective heat transfer coefficient is low at a lower Reynolds number, which makes the cooling of the pin fin dependent on the latent heat of the PCM material. Once the PCM undergoes a phase change, the base temperature increases significantly due to less convection at a lower Reynolds number. The graph shows a similar trend to the base temperature comparison without PCM, but with reduced temperature values, pertaining to the use of PCM. The thermal characteristics of pin fins with PCM material are superior to that of pin fins without PCM. The difference in temperature between the normal pin fin and the PCM pin fin is prominent at lower Reynolds number while this difference reduces at higher Reynolds number.

5. Conclusion

A comparative analysis was carried out among cross flow and jet impingement flow methods to analyze the thermal characteristics of pin fins. Later, a phase changing material was also incorporated into the pin fin system to study the change in operating temperature. A total of 5 different parameters were investigated. The main findings are listed below.

Cross flow proved significantly better characteristics in all aspect. The Nusselt's number was found to increase with the Reynolds number of the flow for both jet impingement and cross flows. The difference between the two techniques is large and remains same throughout the Reynolds number range studied. The cross flow showed an average increase of 41.1% in Nusselt number values as compared to jet impingement over the range of Reynolds number studied.

It is observed that the pressure drop between the two conditions is low at lower Reynolds numbers but it increases significantly for the jet impingement case at higher values. The pressure drop and therefore the power consumption is largely stable through a range of values for the cross flow case. The jet impingement methods demand an average of 61% more pumping power than that of cross flow for the given configuration.

The thermal resistance is also observed to be lower for the crossflow case, it should be noted that the lower pressure drop is favorable since it consumes lesser power. The jet impingement has an average of 41% more thermal resistance than cross flow. As a result, the base temperature under steady state conditions is noticeably lower in the case of cross flows, with an average reduction of 14.5 °C.

The use of PCM significantly reduces the operating temperature of the pin fins by an average of 7.5 °C for cross flow and 6.1 °C for jet impingement flow technique.

Acknowledgments

Authors' Contributions

Deerajkumar Parthipan: Writing, validation and simulation of CFD results. Deepakkumar Rajagopal: Conceptualization, supervision and original draft preparation. Babu Dharmalingam: Review and editing, data collection, data curation and language corrections. Somasundharam Sankaran: Review and editing, data collection, data curation and language corrections.

Disclosure statement

The authors have no competing interests to declare that are relevant to the content of this article. The authors declare that no funds, grants, or other support were received during the preparation of this manuscript.

ORCID

Deepakkumar Rajagopal 🄳 http://orcid.org/0000-0002-4558-1094

References

[1] D. Thesiya, H. Patel and G. S. Patange, "A comprehensive review electronic cooling: a nanomaterial perspective," *Int. J. Thermofluids*, vol. 19, pp. 100382, 2023. DOI: 10.1016/j.ijft.2023.100382.
[2] R. Boukhanouf and A. Haddad, "A CFD analysis of an electronics cooling enclosure for application in telecommunication systems," *Appl. Therm. Eng.*, vol. 30, no. 16, pp. 2426–2434, Nov. 2010. DOI: 10.1016/j.applthermaleng.2010.06.012.
[3] W. X. Chu, M. K. Tsai, S. Y. Jan, H. H. Huang and C. C. Wang, "CFD analysis and experimental verification on a new type of air-cooled heat sink for reducing maximum junction temperature," *Int. J. Heat Mass Transf.*, vol. 148, pp. 119094, Feb 2020. DOI: 10.1016/j.ijheatmasstransfer.2019.119094.
[4] M. A. I. Rashid, M. F. Ismail and M. Mahbub, "CFD analysis in a liquid-cooled carbon nanotube based micro-channel heatsink for electronic cooling," *IJET*, vol. 3, no. 5, pp. 553–559, 2011. DOI: 10.7763/IJET.2011.V3.284.
[5] M. Bahiraei, S. Heshmatian, M. Goodarzi and H. Moayedi, "CFD analysis of employing a novel ecofriendly nanofluid in a miniature pin fin heat sink for cooling of electronic components: effect of different configurations," *Adv. Powder Technol.*, vol. 30, no. 11, pp. 2503–2516, Nov 2019. DOI: 10.1016/j.apt.2019.07.029.
[6] B. Freegah, A. A. Hussain, A. H. Falih and H. Towsyfyan, "CFD analysis of heat transfer enhancement in plate-fin heat sinks with fillet profile: investigation of new designs," *Therm. Sci. Eng. Progr.*, vol. 17, pp. 100458, Jun 2020. DOI: 10.1016/j.tsep.2019.100458.
[7] A. Sarma and A. Ramakrishna, "CFD analysis of splayed pin fin heat sink for electronic cooling." *Int. J. Eng. Res. Technol.*, vol. 1, pp. 1–7, 2012.
[8] V. M. Kulkarni and B. Dotihal, "CFD and conjugate heat transfer analysis of heat sinks with different fin geometries subjected to forced convection used in electronics cooling," *IJRET*, vol. 04, no. 06, pp. 158–163, 2015. DOI: 10.15623/ijret.2015.0406026.
[9] J. K. Kyoung, "Orientation Effects on the Performance of Natural Convection Cooled Hybrid Fins" University of Greenwich and Institute of Electrical and Electronics Engineers," in THERMINIC 2014 : 20th International Workshop, Thermal Investigations of ICs and Systems : proceedings, September 24–26, 2014. Greenwich, London, UK.
[10] H.-Y. Li and K. Chen, "Thermal-fluid characteristics of pin-fin heat sinks cooled by impinging jet," *J. Enhanc. Heat Transf.*, vol. 12, no. 2, pp. 189–202, 2005. DOI: 10.1615/JEnhHeatTransf.v12.i2.40.
[11] S. B. Chin, J. J. Foo, Y. L. Lai and T. K. K. Yong, "Forced convective heat transfer enhancement with perforated pin fins," *Heat Mass Transf.*, vol. 49, no. 10, pp. 1447–1458, 2013. DOI: 10.1007/s00231-013-1186-z.

[12]   K. S. Yang, W. H. Chu, I. Y. Chen and C. C. Wang, "A comparative study of the airside performance of heat sinks having pin fin configurations," *Int. J. Heat Mass Transf.*, vol. 50, no. 23–24, pp. 4661–4667, Nov 2007. DOI: 10.1016/j.ijheatmasstransfer.2007.03.006.

[13]   G. Xie, J. Liu, Y. Liu, B. Sunden and W. Zhang, "Comparative study of thermal performance of longitudinal and transversal-wavy microchannel heat sinks for electronic cooling," *J. Electron. Packag. Trans. ASME*, vol. 135, no. 2, pp. 021008(1–9), 2013. DOI: 10.1115/1.4023530.

[14]   T. Ur Rehman, H. M. Ali, A. Saieed, W. Pao and M. Ali, "Copper foam/PCMs based heat sinks: an experimental study for electronic cooling systems," *Int. J. Heat Mass Transf.*, vol. 127, pp. 381–393, Dec 2018. DOI: 10.1016/j.ijheatmasstransfer.2018.07.120.

[15]   H. A. El-Sheikh and S. v Garimella, "Enhancement of Air Jet Impingement Heat Transfer Using Pin-Fin Heat Sinks," *IEEE Trans. Comp. Packag. Technol.*, vol. 23, no. 2, pp. 300–308, 2000. DOI: 10.1109/6144.846768.

[16]   H. Sivasankaran, G. Asirvatham, J. Bose and B. Albert, "Experimental analysis of parallel plate and crosscut pin fin heat sinks for electronic cooling applications," *Therm. Sci.*, vol. 14, no. 1, pp. 147–156, 2010. DOI: 10.2298/TSCI1001147S.

[17]   S. E. Ghasemi, A. A. Ranjbar and M. J. Hosseini, "Experimental and numerical investigation of circular minichannel heat sinks with various hydraulic diameter for electronic cooling application," *Microelectron. Rel.*, vol. 73, pp. 97–105, Jun 2017. DOI: 10.1016/j.microrel.2017.04.028.

[18]   S. Mahmoud, A. Tang, C. Toh, R. Al-Dadah and S. L. Soo, "Experimental investigation of inserts configurations and PCM type on the thermal performance of PCM based heat sinks," *Appl. Energy*, vol. 112, pp. 1349–1356, 2013. DOI: 10.1016/j.apenergy.2013.04.059.

[19]   S. Lu and K. Vafai, "A comparative analysis of innovative microchannel heat sinks for electronic cooling," *Int. Commun. Heat Mass Transf.*, vol. 76, pp. 271–284, Aug 2016. DOI: 10.1016/j.icheatmasstransfer.2016.04.024.

[20]   R. Pakrouh, M. J. Hosseini, A. A. Ranjbar and R. Bahrampoury, "A numerical method for PCM-based pin fin heat sinks optimization," *Energy Convers. Manage.*, vol. 103, pp. 542–552, Jul 2015. DOI: 10.1016/j.enconman.2015.07.003.

[21]   P. Naphon, L. Nakharintr and S. Wiriyasart, "Continuous nanofluids jet impingement heat transfer and flow in a micro-channel heat sink," *Int. J. Heat Mass Transf.*, vol. 126, pp. 924–932, Nov 2018. DOI: 10.1016/j.ijheatmasstransfer.2018.05.101.

[22]   H. M. Ali and A. Arshad, "Experimental investigation of n-eicosane based circular pin-fin heat sinks for passive cooling of electronic devices," *Int. J. Heat Mass Transf.*, vol. 112, pp. 649–661, 2017. DOI: 10.1016/j.ijheatmasstransfer.2017.05.004.

[23]   A. Arshad, H. M. Ali, S. Khushnood and M. Jabbal, "Experimental investigation of PCM based round pin-fin heat sinks for thermal management of electronics: effect of pin-fin diameter," *Int. J. Heat Mass Transf.*, vol. 117, pp. 861–872, Feb 2018. DOI: 10.1016/j.ijheatmasstransfer.2017.10.008.

[24]   S. Chang, L. Zhang, X. Li, B. Liu, Y. Meng and H. Hu, "Experimental study of novel paraffin-fatty acid eutectic mixtures for thermal management of electronic devices," *J. Energy Storage*, vol. 84, pp. 110846, 2024. DOI: 10.1016/j.est.2024.110846.

[25]   Y. Hui, R. Lei, T. Huang, X. Li and H. Hu, "Experimental investigation on confined jet impingement boiling heat transfer characteristics on metal foam cover," *Appl. Therm. Eng.*, vol. 236, pp. 121806, 2024. DOI: 10.1016/j.applthermaleng.2023.121806.

[26]   C. W. Hirt and B. D. Nichols, "Volume of fluid (VOF) method for the dynamics of free boundaries," *J. Comput. Phys.*, vol. 39, no. 1, pp. 201–225, Jan 1981. DOI: 10.1016/0021-9991(81)90145-5.

[27]   R. Deepakkumar, S. Jayavel and S. Tiwari, "Computational study of fluid flow characteristics past circular cylinder due to confining walls with local waviness," *J. Phys.: Conf. Ser.*, vol. 759, no. 1, pp. 012083, 2016. DOI: 10.1088/1742-6596/759/1/012083.

[28]   R. Deepakkumar, S. Jayavel and S. Tiwari, "Cross flow past circular cylinder with waviness in confining walls near the cylinder," *JAFM*, vol. 10, no. 1, pp. 183–197, 2017. DOI: 10.18869/acadpub.jafm.73.238.26148.

[29]   R. Deepakkumar, S. Jayavel and S. Tiwari, "A comparative study on effect of plain- and wavy-wall confinement on wake characteristics of flow past circular cylinder," *Sadhana*, vol. 42, no. 6, pp. 963–980, 2017. DOI: 10.1007/s12046-017-0649-1.

[30]   R. Deepakkumar and S. Jayavel, "Effect of local waviness in confining walls and its amplitude on vortex shedding control of the flow past a circular cylinder," *Ocean Eng.*, vol. 156, no. March, pp. 208–216, 2018. DOI: 10.1016/j.oceaneng.2018.03.018.

[31]   T. M. Jeng, S. C. Tzeng and H. R. Liao, "Flow visualizations and heat transfer measurements for a rotating pin-fin heat sink with a circular impinging jet," *Int. J. Heat Mass Transf.*, vol. 52, no. 7–8, pp. 2119–2131, Mar 2009. DOI: 10.1016/j.ijheatmasstransfer.2008.10.028.

[32]   P. Deerajkumar and R. Deepakkumar, "Comparative analysis of cross flow and jet impingement techniques of heat sink in electronics cooling," *Mater. Today: Proc.*, vol. 72, no. Part 6, pp. 3081–3088, 2023. DOI: 10.1016/j.matpr.2022.09.251.